Ballistic Experiments on Shock-Induced Combustion in Square Channel

M.V. Doroshko, U.M. Hryshchanka, V.V. Leschevich, O.G. Penyazkov, V.A. Vasetskiy
Physical and Chemical Hydrodynamics Laboratory, Heat and Mass Transfer Institute
220072, Minsk, Belarus

1 Introduction

Shock-Induced Combustion (SIC) is a combustion of a reactive mixture initiated behind the reaction-independent shock wave. From practical perspective, studying this phenomenon is of special importance for solving problems of combustion establishment in supersonic flows regarding high-speed propulsion systems. Therefore, a large bode of the fundamental experimental and numerical researchers were done. Traditionally, work has been divided between blunt body flows, focusing on unsteady phenomena near the Chapman-Jouguet (C-J) point, and wedge flows, with emphasis on oblique detonation wave formation (ODW). Most of experimental studies are carried out by firing a high velocity projectile (HVP) into a quiescent combustible mixture which avoids the problem of supersonic mixing and premature ignition. Varying the geometric and kinematic HVP characteristics and the reactivity of the gas mixture it is possible to observe practically all known types of combustion. For the first time such experiment was realized by Zel'dovich and Leipunskii [1]. In next study [2] Zel'dovich and Shlyapentokh using simple streak photography had already observed the interesting pulsating behavior of the reactive flowfield, which is much more vividly shown in the schlieren photographs of the later investigators [3-8]. The more recent contributions on combustion instabilities produced by HVP come from Japanese groups [8-13]. They reported additional flowfield photographs of different regimes. As other modern studies [14-17], more attention was paid to the problems of ODW initiation and stabilization. Vasiliev [18] and Lee [19] proposed an analytical equation to estimate "direct initiation" critically that was experimentally confirmed for the projectile velocities below and slightly above C-J detonation velocity [14]. Kasahara et al. [20] extended the projectile velocities through approximately 1.8 times of the C-J velocity and proposed a semiempirical critically equation for the stabilization. Furthermore, new unsteady combustion wave structure called "Straw Hat" consisting of SIC region followed by a C-J ODW was observed near the critical conditions [21]. A similar unsteady propagation was reported early by Chernyavskii et al. [22]. Kaneshige and Shepherd [17] visualized a local explosion downstream of a SIC region near a stabilizing criticality of an ODW and described it as an unsteady deflagration-to-detonation transition (DDT) process, but single frame technique has not allowed detailed investigations of temporal evolution of these phenomena. It became available with the introduction of high-speed multi frame cameras in ballistic experiments, and the extensive contribution came again from Japanese researchers. Detailed visualized time histories of "Straw Hat" combustion propagation [10, 11] allowed to divide it in two propagation types: with stabilized and attenuated ODW. The one type was that the bow shock and the unsteady SIC region were coupled near the projectile until reaching the transition point at certain downstream, and they were connected to the ODW region. General flowfield and the conical ODW faraway from the projectile were almost steadily, but the transition points were unsteady: the ODW gradually slid back relative to the projectile as the time increases until repeating strong local explosions in the SIC region near the transition point moved the ODW front upstream. As this flowfield didn't be disrupted instantaneously and had almost constant wave structure during passing the observation region it was classified as stable phenomena. The mechanism of the ODW sustaining was proposed to be connected with local explosions that apparently differ from DDT process observed by Kaneshige and Shepherd [17]. According to the Maeda et al. [11] in experiments of Kaneshige and Shepherd the parts of observed ODWs were over-driven due to Mach reflections with the chamber wall and the effects of chamber wall on stabilizing ODWs were considerable because of low facility aspect ratio (relation between dimensions of test chamber and projectile). Only a few kilopascal difference in filling pressure divided the Straw Hat type with a stabilized ODW from that with an attenuated. The bow shock and unsteady SIC region become decoupled at some distance from projectile and are connected to the ODW without the local explosions. Therefore, the transition point continuously moves away from the projectile and gradually disappeared over time [11]. Previously obtained observations of Kasahara et al. [9] revealed that the projectile entrance phenomena at the chamber inlet (a diaphragm rupture or a muzzle jet from a barrel) was responsible for detonation initiation and Straw Hat type with attenuated ODW was considered as transition to SIC mode.

From the above consideration it seems like the problem of ignition by the shock wave generated by a HVP travelling in a reactive gas mixture is completely studied. All unique experimental data were well interpreted by high time and spatial resolution optical observation, have received an adequate theoretical description and were verified by numerical calculations. But the influence of some facility-dependent nonideal effects were studied at less, although it was often noted that they could initiate a detonation, even when HVP itself would not. The projectile entrance phenomena were observed and partially studied in [9]. In [14] by using diaphragms of different thickness no effect on detonation initiation was observed. But in the same facility some experimental results were found sensitive to the existence of a buffer of inert gas before main diaphragm [15]. As entrance phenomena is a priori unsteady it hasn't practical perspective and is usually carefully isolated from experimental results by increasing the distance to observation region. The wave interactions with the walls of the chamber is also avoided by increasing its dimensions relative to projectile size. The final phenomenon in our opinion is more interesting for practical applications since in real devices combustion is always organizing in a certain volume limited by walls and direct or additional combustion initiation can be achieved in the reflection region. The possibility of this was noted by Lee [19] and even observed in experiments [17, 23] as intermediate phenomena. This inspires confidence that the presence of a walls parallel to the axis of flying HVP at some distance can cause the initiation and stabilization of combustion under previously unreachable conditions (lower pressure and higher Mach number). It became the main idea for current experimental study. On best of our knowledge only one similar work was carried out to date [15]. The effect of confinement was evident but investigated only on the initiation of detonation waves at projectile velocities below C-J in cylindrical tube and without combustion visualization.

2 Ballistic experiment description and experimental conditions

The experimental setup is shown Fig.1. The projectile was accelerated in the barrel of a hybrid two-stage launcher developed at A.V. Luikov Heat and Mass Transfer Institute of the National Academy of Sciences of Belarus [24, 25]. The device consists of a pulsed erosive plasma generator (first stage), a high-pressure light-gas section with a plastic piston (second stage), and an acceleration barrel. The barrel and the high-pressure section have inner diameter 6 and 13 mm, length 300 and 760 mm, respectively, and are divided by brass diaphragm. The launcher is capable to achieve velocities up to 3 km/s for 0.12 g weight projectiles by varying initial voltage of plasma generator power supply.

The observation chamber (test section) has a 35 mm square cross-section, a length 370 mm and quartz windows 200x35 mm installed at 35 mm distance from chamber entrance. At the inlet and outlet of the chamber, round diaphragms with a diameter of 35 mm were made from two layers of a 10 μm thickness Lavsan (Mylar). Test chamber mainly for safety reasons was installed in hermitical closed diagnostic chamber which also allows to change ambient gas and its pressure from atmospheric to

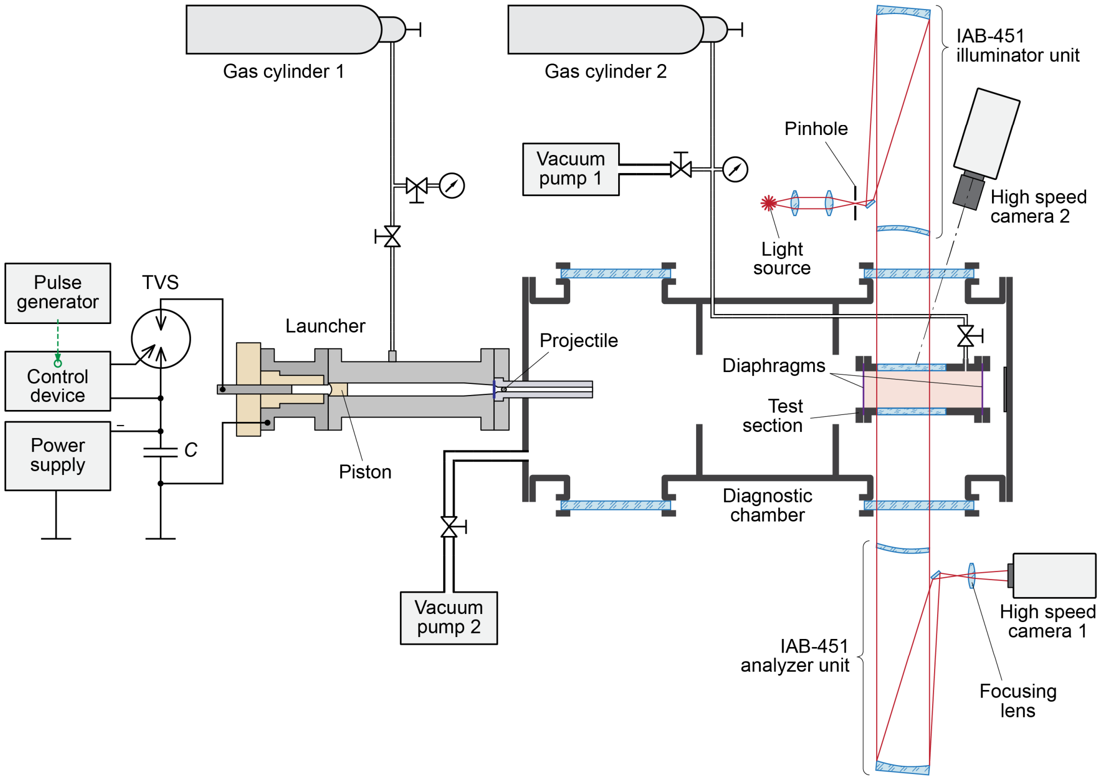

Figure 1: Schematic diagram of the experimental arrangement (top view)

medium vacuum. The used in this study distance between a barrel exit and test section entrance of 680 mm and atmospheric pressure of air inside diagnostic chamber isolated experimental results from the muzzle blast wave and small debris as they were quickly decelerated. Spherical projectiles were chosen to eliminate the difficulty of zero angle attack orientation. We used standard 6 mm in diameter airsoft bullets because of calibrated size, weight and sufficient strength (on average 1 from 15 shorts was destroyed). They made of heavy plastic and were launched without sabot with using only thin cellophane film for additional sealing inside the barrel. Therefore, some debris (fragments of cellophane or brass diaphragm, erased parts of bullet and barrel) always escort projectile on close to the muzzle distances.

Test section before experiment was evacuated to residual pressures less than 10 Pa and filled with test mixture to a given initial pressure from a storage cylinder with accuracy ± 0.2 kPa. The stoichiometric acetylene-oxygen mixture with 55 % nitrogen dilution was preliminarily prepared by the partial pressure method from high-purity individual gases (99.95-99.99%) with accuracy ±0.51 %, ±0.11 % and ±0.12 % for C_2H_2, O_2 and N_2 components, respectively, and kept several days to complete mix by molecular diffusion. The C-J detonation velocity ($D_{C\text{-}J}$) for each initial pressure was calculated by own chemical equilibrium software using thermodynamics database [26]. To express the critically conditions needed to direct initiation [19] and stabilization [20] of a detonation wave around the projectile, it is necessary to know the detonation cell size λ. Usually fitting equations for experimental data collected by Kaneshige and Shepherd [27] were using by other researchers. But for studded here mixture composition there are no direct λ measurements. Therefore, we used fitting equations previously obtained from experimental data [28, 29] on critical diameter for acetylene detonation diffraction using 13λ criteria in the form:

$$\lambda = A \cdot P_0^{-1.1} \qquad (1)$$

where coefficient A depends on nitrogen/oxygen ratio (β): 24.6 at β=0, 225.1 at β=1.4 and 1608.2 at β=3.76, initial pressure (P_0) in kilopascals and cell size (λ) in millimeters. For our diluted on 55% with N_2 mixture β=1.71 and A was interpolated as 3301.

During the experiment two high-speed video Photron FASTCAM SA-Z cameras (112 kfps speed, 160 ns exposure time and 896x184 pixels resolution) were used for shadowgraph and natural emission records. Cameras were arranged like shown on Fig.1: for shadowgraph perpendicular to axis and natural light at the angle of 78° to oncoming projectile motion. The shadowgraph imaging system for observation of wave structure was conventional device IAB-451 [30] consisted of illuminator and analyzer units. A light from mercury lump with modified power supply was used as a point light source (a pinhole is 1 mm). A field of view of this system is even large than our observation windows. A focusing lens f=0.22 m was used to construct a shadowgraph image on the camera CCD sensor. The projectile velocity was determined using subsequence shadowgraph images as the gradient of straight line passing the first and last points of its location in the observation region. A spatial resolution of each image is 0.1838 mm/pixel, but due to a fuzzy projectile image a location of its center was measured with accuracy ±0.55 mm. Taking into account decelerating of projectile during observation time the relative error of presented in this paper velocities is about 1% of measured value.

3 Shadowgraphs of different combustion regimes and discussion

All tested experimental conditions and results are listed in Table 1. Varying filling test chamber pressure (P_0) and projectile velocity (V_P) we registered different combustion regimes during observation time on distance of 165 mm started at 35 mm from channel entrance. We divided them in 4 types depending on stationarity of registered flowfield.

Table 1: Experimental conditions and results.

Test Mixture	P_0, kPa	V_P, m/s	$D_{C\text{-}J}$, m/s	Result	Fig.
C_2H_2+2.5O_2+4.28N_2	98	1800	2049	Outrunning detonation	2a
	88.9	1900	2046		
	90	1980	2047		
	89.1	1980	2047		2b
	89.6	2000	2047		
	81	2000	2043		
	80.3	2020	2043		2c
	79.7	2350	2042	Trailing detonation	3a
	81.9	2620	2044		3b, 4a
	50.2	2640	2027		3c
	91.5	2830	2048		4b
	90.5	2060	2047	Stabilized detonation	4c
	100	2110	2051		
	98.5	2660	2049		
	98.4	2910	2049		
	98.2	2930	2049		
	99.2	3130	2050		
	20	2660	1995	Shock-induced combustion	
	5	2700	1947		
	5	3060	1947		

When V_P is lower than $D_{C\text{-}J}$ a planar stationary detonation wave develops in front of projectile and runs upstream at C-J velocity. The distance and time it takes depend on projectile velocity and the formation mechanism is sensitive to filling pressure and distance from traveling axes to the channel wall. At atmospheric pressure (Fig. 2a) we see that accelerating and straightening of the initiated just after entrance reaction front (coupled with bow shock) occurs simultaneously above and under the axis of projectile flight. In a top region it is caused by a sequence of downstream strong local explosion while in a bottom that closer to the channel's wall a straightening proceeds continuously and more quickly before the blast wave reaches it. At lower pressures an unsteady SIC around projectile decoupled from bow shock can be found (Fig. 2b). Local explosions at top and bottom walls (probably in the corners where mixture was heated but not ignited) are responsible for detonation initiation. With decreasing pressure and increasing projectile velocity a process of a planar detonation wave formation is delayed and doesn't appear during observation time (Fig. 2c). We believe that it will be happened since local explosions near walls continuously escorts projectile flight.

For V_P higher than D_{C-J} and filling pressure 50-80 kPa shock-induced combustion with following detonation wave was observed. From Fig.3a (only shadowgraph image is available) we suggest that this detonation process starts from strong local explosion just after projectile entrance and propagates near the walls in heated and unreacted mixture appeared there due to splitting of bow shock and reaction front. The slope of the detonation wave is related to the deviation of the projectile's travel axis from the center of the channel that caused a gas near the bottom wall to be heated earlier. It is steady phenomena but as its velocity lower than projectile one this wave continuously lags and will not fall in observation area at long distances. Therefore, we classified this regime as unstable and called as "Trailing detonation".

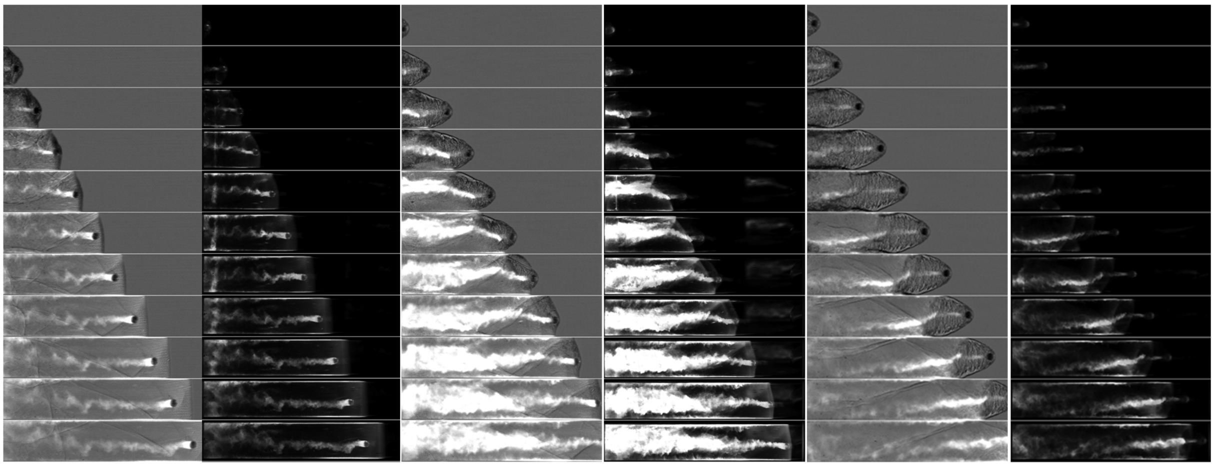

a b c

Figure 2: Outrunning detonation shadowgraph image (left) and chemiluminescence (right)

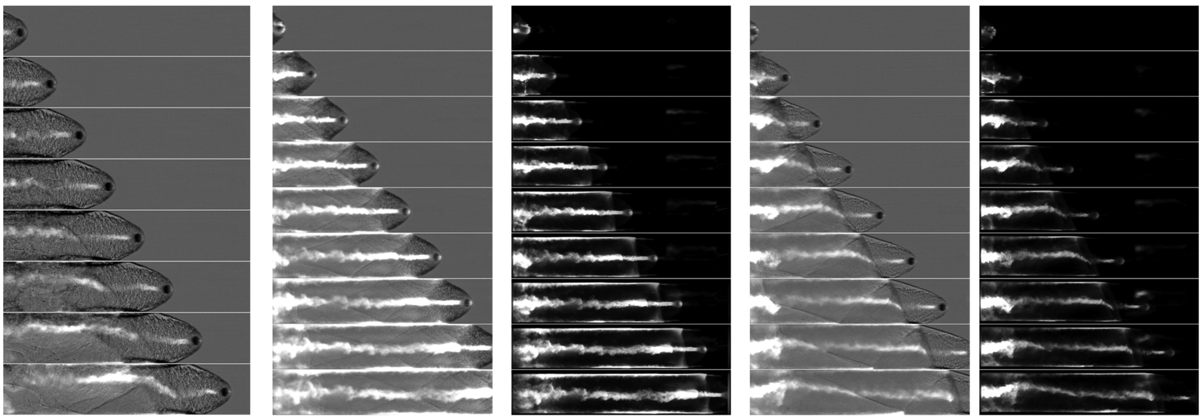

a b c

Figure 3: Trailing detonation shadowgraph image (left) and chemiluminescence (right)

A flowfield presented in Fig.3b was filmed under the similar pressure as in Fig.3a, but when projectile traveled close to the channel axis with higher velocity. No wave splitting is observed and reaction coupled to bow shock. It looks like stabilized conical detonation wave but the points of contact with the walls gradually shift downstream (Fig. 4a right) and the normal velocity component of wave decreases from 0.75 to 0.58 of C-J value. The reflection pattern near walls resembling a Mach reflection disappears during the observation time. Therefore, we classified this regime as unstable but it is close to critical, because at higher pressure and similar projectile velocity (Fig. 4c) higher normal velocity component was detected with increasing from 0.89 to 0.9 of C-J value during observation. This regime is close to described in [11] as a stabilized ODW with unsteady region. The difference from our case is that wave reflection from the wall replaces the effect of unsteady local explosions accelerated the normal velocity component to C-J value. Therefore, this regime is can be considered as stabilized. The critically of projectile velocity for stabilization of supersonic combustion mode in channel at close to atmospheric pressure is evident from Fig.4b. Opposite to case presented in Fig. 4a we can see how “Mach reflection” pattern near the top wall forms during time and local normal velocity component increases from 0.9 to 1.2 of the C-J value. This regime resembles a Straw Hat type with a stabilized ODW [11], that was classified as transitional to stable ODW. From our observations it is seen that unsteady region near top wall gradually slides downstream therefore we consider this combustion propagation as unstable and close to critical. Probably, the wave front curvature near the inflection point appeared in a top part of last two frames is the initiation of a local explosion, which in the case of a Straw Hat type with a stabilized ODW regime is a source of stabilizing mechanism. But we didn’t detect this scenario and only can suppose it. Nevertheless, flowfield near a bottom wall that closer to the projectile travel axis remains steady. This indicates that the distance to the wall can become new criterion for combustion stabilization.

Finally, at pressure 20 kPa and lower no detonation wave development was detected for projectile velocities higher C-J value. A sharp splitting of the shock wave and the reaction front near the projectile was observed, so combustion occurs only in the central part of the channel in a gas column (or only on its surface) with a diameter of about three projectile diameters. Combustion near the channel’s walls was started at some distance from the point of bow shock reflection. It was clear that mixture was not fully reacted behind projectile, because new ignition front was observed behind the reflected from channel exit shock wave. Ignition at pressure 5 kPa was probably caused by entrance phenomena because combustion slowly propagated to the channel exit. The shadowgraph and chemiluminescence images filmed in these experiments are not presented here due to very low contrast. These unsteady regimes were classified as SIC and their conditions are considered as close to ignition limits.

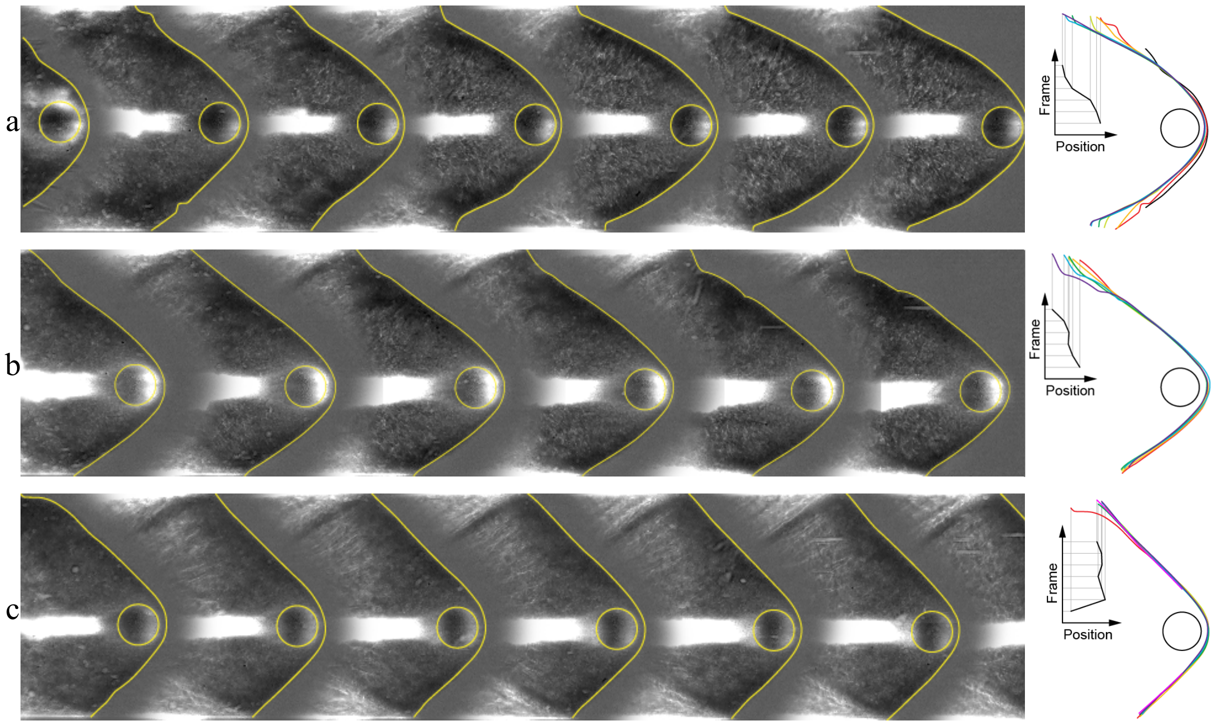

Figure 4: Stabilized detonation regime determination by shadowgraph images contouring (left) and superposition (right)

4 Concluding remarks

All studied conditions and their results are graphically shown in Fig. 6 as dependence of projectile velocity (Mach number of flow) on a mixture filling pressure (left). In order to compare conditions of stabilized regimes with the Lee's initiation [19] and Kasahara's stabilization [20] criteria them were also expressed by the non-dimensional projectile diameter and velocity (right). It made evident why no detonation waves were developed during low pressure experiments. The discovered stabilized combustion modes are significantly lower than even initiation criteria line. We connect it with observed wall effect but not exclude inaccuracy of used fitting equation (1) for cell size calculations.

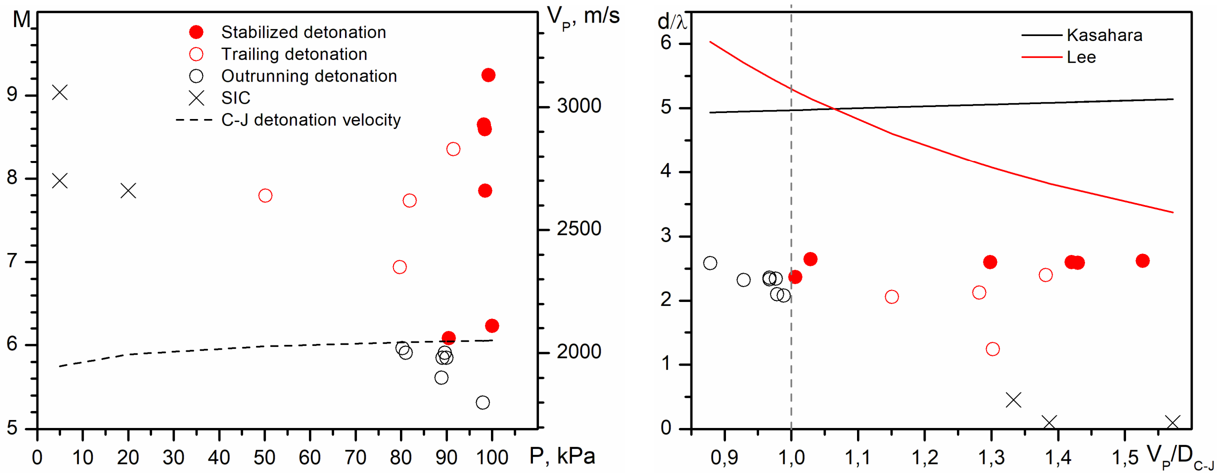

Figure 6: Combustion regimes conditions (left) and comparison with different criteria (right)

Acknowledgements

The authors gratefully acknowledge the financial contribution from NAS of Belarus (grant EP-2.13)

References

[1] Zel'dovich YaB, Leipunskii OI. (1943). A study of chemical reactions in shock waves - theory of the method and results of the preliminary experiment. O.Acta Physicochimica URSS. 18(2-3):167-171.
[2] Zel'dovich YaB, Shlyapintokh IYa (1949). Ignition of explosive gas mixtures in a shock wave. Dokl.Akad. Nauk SSSR. 115(6): 871-874.
[3] Ruegg FW, Dorsey WW. (1962). A missile technique for the study of detonation waves. Journal of Research of the National Bureau of Standards - C. Engineering and Instrumentation. 66C(1): 51–58.
[4] Behrens H, Struth W, Wecken F. (1964) Studies of hypervelocity firings into mixtures of hydrogen with air or with oxygen. Proc. Combust. Inst 10: 245–252.
[5] Cheryni GG. (1967). Supersonic flow past bodies with generation of detonation and slow combustion fronts. Acta Astronaut. 13: 464-480.
[6] Alpert RL, Toong TY. (1972). Periodicity in exothermic hypersonic rows about blunt projectiles. Astronaut. Acta 17: 539-560.
[7] Lehr HF. (1972) Experiments on shock-induced combustion. Astronaut. Acta. 17(4, 5): 589-597.
[8] Kasahara J, Horii T, Endo T, Fujiwara T. (1996). Experimental observation of unsteady H2-O2 combustion phenomena around hypersonic projectiles using a multiframe camera. Proc. Combust. Inst. 26(2):2903–2908.
[9] Kasahara J, Fujiwara T, Endo T, Arai T. (2001)/ Chapman–Jouguet oblique detonation structure around hypersonic projectiles. AIAAJ. 39(8): 1553–1561.

[10] Maeda S, Inada R, Kasahara J, Matsuo A. (2011) Visualization of the non-steady state oblique detonation wave phenomena around hypersonic spherical projectile. Proc. Combust. Inst. 33: 2343–2349.
[11] Maeda S, Kasahara J, Matsuo A. (2012). Oblique detonation wave stability around a spherical projectile by a high time resolution optical observation. Combust. Flame. 159 (2): 887-896.
[12] Maeda S, Sumiya S, Kasahara J. (2015) Scale effect of spherical projectiles for stabilization of oblique detonation waves. Shock Waves 25:141–150.
[13] Maeda S, Kanno S, Yoshiri I, Obara T. (2017) Time-resolved schlieren observations of shock-induced combustion around a high-speeds spherical projectile. Sci. Tech. Energenic Materials. 78 (1): 19-26.
[14] Higgins AJ, Bruckner AP. (1996). Experimental investigation of detonation initiation by hypervelocity blunt projectiles. AIAA paper 96-0342.
[15] Higgins AJ. (1997). The effect of confinement on detonation initiation by blunt projectiles. In 33rd AIAA/ASME/SAE/ASEE Joint Propulsion Conference and Exhibit, number AIAA-97-3179, Seattle, WA.
[16] Verreault J, Higgins AJ. (2011). Initiation of detonation by conical projectiles. Proc. Combust. Inst. 33: 2311–2318.
[17] Kaneshige MJ, Shepherd JE. (1996). Oblique detonation stabilized on a hypervelocity projectile. Proc. Combust. Inst. 26: 3015–3022.
[18] Vasiljev AA. (1994) Initiation of gaseous detonation by a high speed body. Shock Waves 3: 321–326.
[19] Lee JHS. (1997). Initiation of detonation by a hypervelocity projectile. Prog. Astronaut. Aeronaut. 173: 293–310.
[20] Kasahara J, Arai T, Chiba S, Takazawa K, Tanahashi Y, Matsuo A. (2002) Criticality for stabilized oblique detonation waves around spherical bodies in acetylene/oxygen/krypton mixtures. Proc. Combust. Inst. 29: 2817–2824.
[21] Kasahara, J., Endo, T., Nishide, K., Yahata, D., Yoshikawa, N., and Fujiwara, T., Proc. Int. Symp. Shock Waves 22:303 (1999).
[22] Chernyavskii SYu, Baulin NN, Mkrtumov AS. (1973). High-speed flow of a mixture of hydrogen and oxygen over blunt bodies. Combust. Expl. Shock Waves 9: 687–690.
[23] Benedick WB. (1982). Review of large scale fuel-air explosion tests and techniques. In J.H.S. Lee and C.M. Guirao, editors, Fuel-Air Explosions: 507–552.
[24] Khramtsov PP, Penyazkov OG, Vasetskii VA, Grishchenko VM, Makhnac, A., Shikh IA. (2015). Physical principles of operation of a two-stage light gas magnetoplasma launcher for high-vacuum ballistic tests. J. Eng. Phys. Thermophys. 88(5): 1118–1126.
[25] Doroshko MV, Hryshchanka U, Leschevich VV, Makhnach AI, Vasetskiy VA. (2022) Improvement of ballistic launcher characteristics for solid macroparticles acceleration // High Temperature Material Processes: An International Quarterly of High-Technology Plasma Processes. 26(4): 39–51.
[26] Kee RJ, Rupley JA, Miller FM. (1994). The chemkin thermodynamic data base. Sandia Technical Report SAND87-8215B, UC-4, Sandia National Laboratories, Livermore, CA.
[27] Kaneshige MJ, Shepherd JE. (1997). Detonation database, GALCIT Technical Report FM97-8. http://www.galcit.caltech.edu/detn_db/html/.
[28] Matsui H, Lee JH. (1978). On the measure of the relative detonation hazards of gaseous fuel-oxygen and air mixtures. Proc. Combust. Inst. 17: 1269–1279.
[29] Knystautas R, Lee JH, Guirao CM. (1982). The critical tube diameter for detonation failure in hydrocarbon-air mixtures. Combust. Flame 48: 63–83.
[30] Settles GS. (2001). Schlieren and shadowgraph techniques: Visualizing phenomena in transparent media. Springer-Verlag, Berlin: 195–197.